Synthesis and Characterization of Crystalline Graft Polymer Poly(ethylene oxide)-*g*-poly(ε-caprolactone)$_2$ with Modulated Grafting Sites

Yingying Ma,[1,2] Jian Huang,[2] Kunyan Sui,[1] Guowei Wang[2]

[1]Department of Polymer Science and Engineering, State Key Laboratory Cultivating Base for New Fiber Materials and Modern Textiles, Qingdao University, Qingdao 266071, China
[2]Department of Macromolecular Science, State Key Laboratory of Molecular Engineering of Polymers, Fudan University, Shanghai 200433, China
Correspondence to: K. Sui (E-mail: kunyansui@163.com) or G. W. Wang (E-mail: gwwang@fudan.edu.cn)

Received 31 March 2014; accepted 1 May 2014; published online 23 May 2014
DOI: 10.1002/pola.27239

ABSTRACT: The graft polymer poly(ethylene oxide)-*g*-poly(ε-caprolactone)$_2$ (PEO-*g*-PCL$_2$) with modulated grafting sites was synthesized by the combination of ring-opening polymerization (ROP) mechanism, efficient Williamson reaction, with thiol–ene addition reaction. First, the precursor of PEO-Allyl-PEO with two terminal hydroxyl groups and one middle allyl group was prepared by ROP of EO monomers. Then, the macroinitiator [PEO-(OH)$_2$-PEO]$_s$ was synthesized by sequential Williamson reaction between terminal hydroxyl groups and thiol–ene addition reaction on pendant allyl groups. Finally, the graft polymer PEO-*g*-PCL$_2$ was obtained by ROP of ε-CL monomers using [PEO-(OH)$_2$-PEO]$_s$ as macroinitiator. The target graft polymer and all intermediates were well characterized by the measurements of gel permeation chromatography, ^{1}H NMR, and thermal gravimetric analysis. The crystallization behavior was investigated by the measurements of differential scanning calorimetry, wide-angle X-ray diffraction and polarized optical microscope. The results showed that when the PCL content of side chains reached 59.2%, the crystalline structure had been dominated by PCL part and the crystalline structure formed by PEO part can be almost neglected. © 2014 Wiley Periodicals, Inc. J. Polym. Sci., Part A: Polym. Chem. **2014**, *52*, 2239–2247

KEYWORDS: crystallization; graft polymer; poly(ε-caprolactone) (PCL); poly(ethylene oxide) (PEO); ring-opening polymerization (ROP); Williamson reaction; thiol-ene addition reaction

INTRODUCTION With the rapid development of living/controlled polymerization mechanisms and efficient coupling methods, a variety of polymers with complicated architectures and compositions can be realized by certain synthetic route. The increasing attention on these complicated architectures is mainly owing to their unique physical properties in solution and bulk, as well as their versatile applications, including biomedical materials,[1,2] nanotechnology,[3] composite materials,[4] and supramolecular science.[5] Among them, the graft polymers are especially paid much attention because there are many parameters that can be modulated in this kind of structure. Usually, the variations of compositions and length of main chains and side chains, as well as the grafting density, have great impacts on bulk physical and mechanical properties of graft polymers.[6] For example, the structures of side chains and main chains of graft copolymers can be designed as block,[7] hyperbranched,[8] V-shaped,[9,10] star-shaped,[11,12] dendrimer-like,[13–15] and so forth. The compositions can be selected from a series of polymers, such as poly(isoprene) (PI),[16,17] poly(ethylene oxide) (PEO),[18] polystyrene (PS),[19–21] poly(acrylic acid),[22] poly(hydroxyethyl methacrylate),[23,24] poly(ε-caprolactone) (PCL),[25] and so on. All these variations make it possible to design and synthesize the aimed graft polymers with certain applications.

Typically, the graft polymers can be realized by "grafting from,"[26–28] "grafting onto"[29–31] or "grafting through"[32–34] strategies. However, each strategy has its own advantages and limitations. For example, in "grafting onto" strategy, the efficient click reactions are usually adopted and the polymers with defined side chains or main chains can be synthesized,[35–37] but the grafting efficiency is sometimes limited. In "grafting from" strategy, the grafting efficiency could reach almost 100%[26,27]; however, the length of side chains cannot be well controlled. In general, in the above three strategies to graft polymers, the design and synthesis of main chain is always the key step. The main chain can not only provide controlled grafting sites, but also can modulate the properties of final graft polymers. For example, PEO is a classical soft segment in multiconstitution polymers, and might endow the polymers with special properties owing to its

Additional Supporting Information may be found in the online version of this article.

good solubility both in water and in organic solvents.[38–40] The polymers contained PEO segments showed potential applications in high energy density lithium batteries, electronic devices,[41] and drug delivery systems,[42] which are receiving increasing interests.[43–45] However, until recently, the PEO segments are difficult and rarely constructed into the main chain of graft copolymers. Previously, Huang and coworkers[18,30,46–57] have explored a method to synthesize functional PEO from the ethoxyethyl glycidyl ether or 4-glycidyl-2,2,6,6-tetra methylpiperidyl-1-oxyl (GTEMPO) monomers, and some graft polymers or sun-shaped polymers have been realized from the PEO backbone pendant with hydroxyl groups or TEMPO groups. However, the monomers for functional PEO main chain are always limited by complicated synthetic procedure of epoxides with substituent groups, and the molecular weights of PEO backbone are always limited $<$20,000 g/mol because of the transfer reactions of living species to epoxide monomers in ring-opening polymerization (ROP) mechanism.

On the other hand, the length between adjacent grafting sites on graft polymers is always modulated by several monomer units, and the grafting sites are rarely separated by a polymer segment with certain length or molecular weight. As a pioneering work, Hadjichristidis et al.[58,59] synthesized some graft polymers PI(or PS)-*g*-PS by living anionic polymerization, in which the grafting sites are separated by the segments of PI or PS. Their results had shown that the physical properties of such graft polymers can be well controlled by modulating the length of spaced segments on main chain. Thus, the synthesis of this kind of graft polymers and the related works need to be further developed.

In this contribution, considering the aforementioned limitation on graft polymers, we aimed to synthesize some graft polymers with PEO as main chain. The modulated grafting sites are specially spaced with a certain length of PEO segment. Also, considering that the PCL segments have been extensively used as an important biomaterial for a wide variety of drug delivery carriers and biomedical devices because of its biodegradability and biocompatibility,[60] as well as composite material because of its versatile mechanical properties and miscibility toward some commodity polymers, we also designed the PCL segments as side chains. In synthetic route, the "grafting from" strategy was adopted, and the ROP mechanism, Williamson reaction with thiol–ene addition reaction were well combined (Scheme 1). Furthermore, because both PEO and PCL were all crystalline segments in target graft polymer PEO-*g*-PCL_2, the crystallization behavior of graft polymer was also investigated.

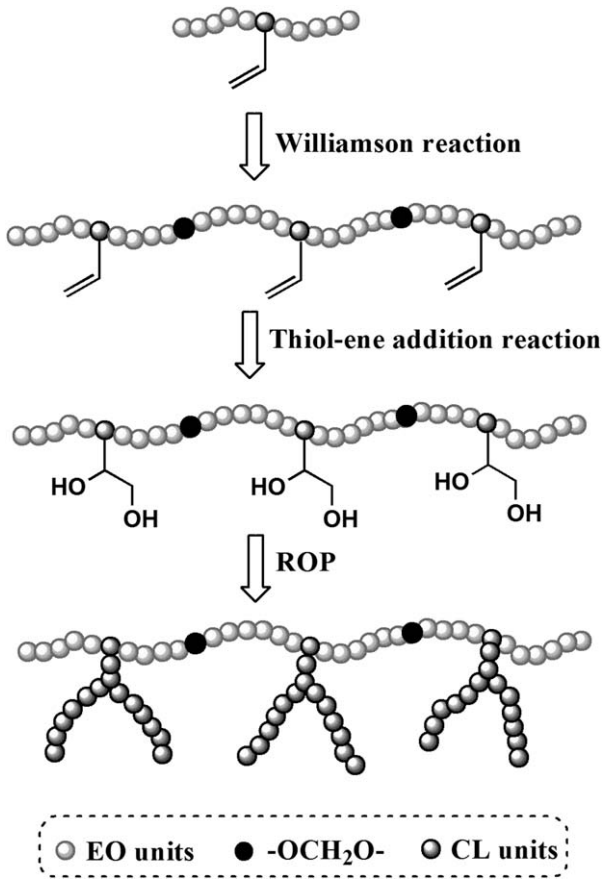

SCHEME 1 The illustration of graft polymer PEO-*g*-PCL_2 and their synthetic procedure.

EXPERIMENTAL

Materials

Ethylene oxide (EO, Sinopharm Chemical Reagent (SCR), 98%) was dried by calcium hydride (CaH_2) for 48 h and then distilled under N_2 before use. ε-Caprolactone (CL) (99%, Aldrich) was purified by distillation from CaH_2 under reduced pressure and stored at -20 °C before use. Tetrahydrofuran (THF, 99%, SCR) was refluxed and distilled from potassium naphthalenide solution. Dichloromethane (CH_2Cl_2, SCR, 98%) and toluene were purified by distillation from CaH_2. Tin (II) *bis*(2-ethylhexanoate) ($Sn(Oct)_2$, 95%, Sigma) was dissolved in dry toluene (0.5 mg/mL). Diphenylmethyl potassium (DPMK) solution with concentration of 0.75 mol/L was prepared according to the literature.[61] All other reagents and solvents were purchased from SCR and used as received except for declaration.

Characterization

Gel permeation chromatographic (GPC) measurement of PEO homopolymers was performed in 0.1 M of $NaNO_3$ aqueous solution at 40 °C with an elution rate of 0.5 mL/min on an Agilent 1100 equipped with a G1310A pump, a G1362A refractive index detector, and a G1315A diode-array detector. Three TSK gel PW columns in series (molecular weight ranges from 0 to 5×10^4 and 5×10^4 to 8×10^6 g/mol) were calibrated with PEO standards. The measurement of GPC of graft polymer poly(ethylene oxide)-*g*-poly(ε-caprolactone)$_2$ (PEO-*g*-PCL_2) was carried out at 35 °C using LiBr-added dimethylformamide (DMF) ([LiBr] = 15 mM) as eluent with a flow rate of 1.0 mL/min. The system was calibrated with linear PMMA standards. The ultrafiltration membrane

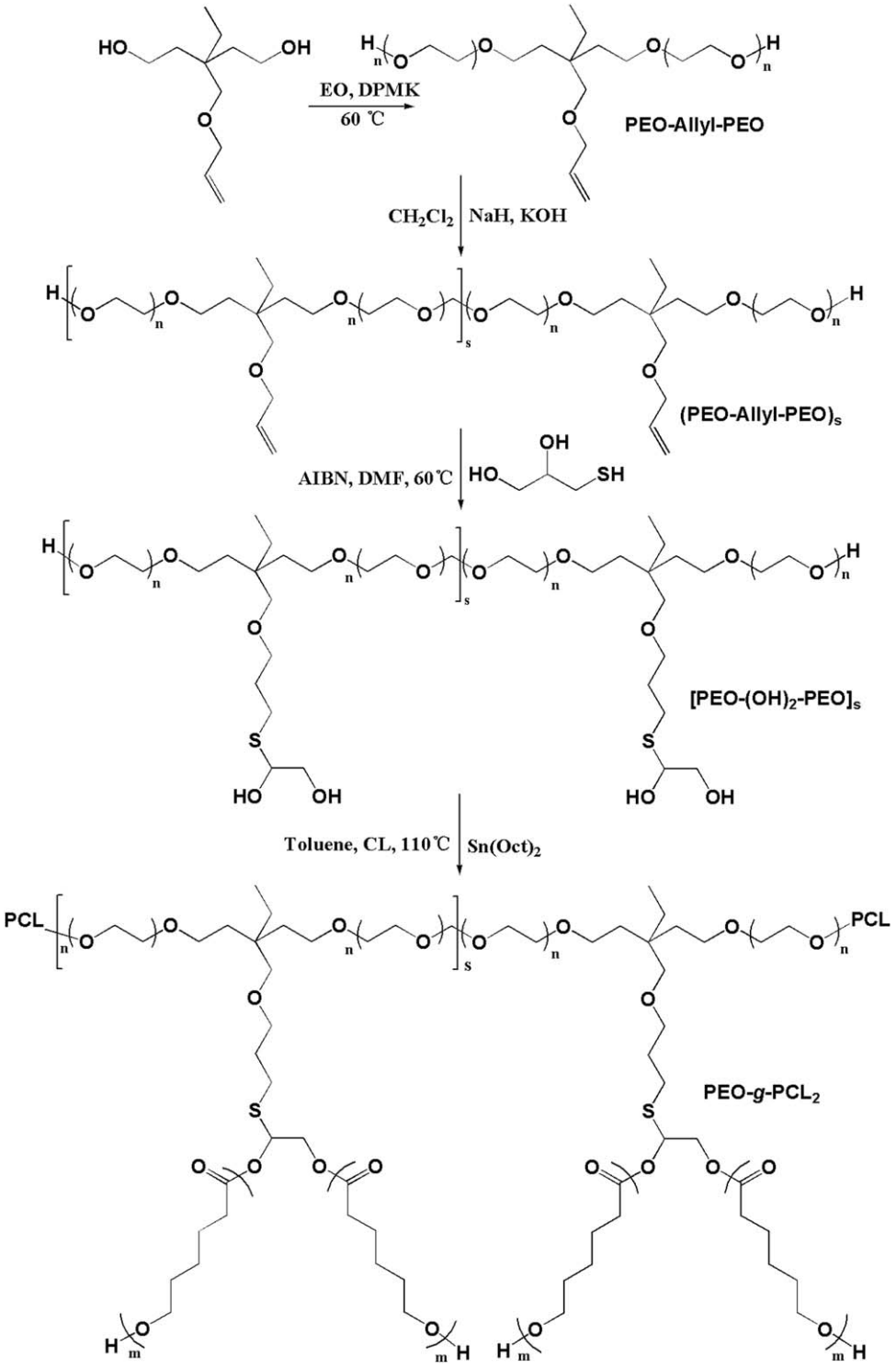

SCHEME 2 The synthetic procedure of graft polymer PEO-*g*-PCL_2.

separator was purchased from Shanghai Institute of Applied Physics, Chinese Academy of Science, and the cut-off molecular weight of used poly(ether sulfone) film was $M_{w(cut\text{-}off)}$ = 10,000 g/mol (calibrated with globin). ^{1}H NMR spectra were recorded on a Bruker (500 MHz) spectrometer in $CDCl_3$ solvent with tetramethylsilane as internal reference. Differential scanning calorimetry (DSC) was carried on a DSC Q2000 thermal analysis system (Shimadzu, Japan). Samples were first heated from −20 to 120 °C at a heating rate of 10 °C/min under nitrogen atmosphere, followed by cooling to −20 °C at 10 °C/min after stopping at 120 °C for 3 min, and finally heating to 120 °C at 10 °C/min after stopping at

−20 °C for 3 min. Thermal gravimetric analysis (TGA) curves were obtained using a Perkin Elmer Pyris 1 at a heating rate of 10 °C/min under nitrogen atmosphere. The measurement of X-ray diffraction (XRD) was carried out using an X9Pert PRO (PANalytical) with Cu Kα (1.541 Å) radiation (40 kV, 40 mA). Samples were exposed at a scanning rate of $2\theta = 5$ °C/min between 2θ values of 10 and 40°. Crystal growth was observed under a polarized optical microscope (POM, Leica, DM 2500P) equipped with a hot stage (Linkam, THMS600) and a CCD video camera.

Synthesis of Precursor with Two Terminal Hydroxyl Groups and One Middle Allyl Group (PEO-Allyl-PEO) by ROP Mechanism (Scheme 2)

The precursor of PEO-Allyl-PEO was synthesized by ROP of EO monomers in dry THF using 3-[(allyloxy)meth-yl]-3-ethyl-1,5-pentanediol as initiator. First, the initiator 3-[(allyloxy)methyl]-3-ethyl-1,5-pentan-ediol (1.50 g, 7.43 mmol) dried by azeotropic distillation with toluene was dissolved in 250 mL dry THF and introduced into a 400-mL ampoule. Then, the DPMK solution (8.00 mL, 6.00 mmol) was added into the ampoule to change —OH into $—O^-K^+$. Subsequently, the EO monomers (21.0 mL, 0.416 mol) were injected into the ampoule rapidly and the reaction was carried out at 60 °C for 72 h. After the polymerization was terminated by methanol (5.0 mL), the system was concentrated and the product was precipitated thrice from cold diethyl ether. The obtained PEO-Allyl-PEO was dried under vacuum at 45 °C for 24 h.

^{1}H NMR ($CDCl_3$) δ (ppm): 0.82 ppm (CH_3CH_2-), 1.22 ppm ($—OCH_2CH_2C—$), 1.37 ppm (CH_3CH_2-), 3.20–3.93 ppm ($CH_2=CHCH_2O—$, $—CH_2CH_2O—$), 5.07–5.27 ppm ($CH_2=CH—$), 5.79–5.91 ppm ($CH_2=CH—$) (See Figure S1 in Supporting Information). $M_{n,NMR} = 4{,}700$ g/mol, $M_{n,GPC} = 4{,}800$ g/mol, and PDI = 1.20.

Synthesis of High-Molecular-Weight (PEO-Allyl-PEO)$_s$ by Williamson Reaction (Scheme 2)

The high-molecular-weight (PEO-Allyl-PEO)$_s$ was synthesized by Williamson reaction between active hydroxyl groups at the end of PEO-Allyl-PEO. Typically, the precursor PEO-Allyl-PEO (35.50 g, 17.75 mmol) dried by azeotropic distillation with toluene was dissolved in 120 mL dry CH_2Cl_2 in a 500 mL round-bottomed flask. Then, the sodium hydride (NaH, 0.10 g, 4.17 mmol) and potassium hydroxide (KOH, 7.00 g, 125.00 mmol) were added and the reaction was carried out at reflux temperature for 72 h. The system was finally evaporated and extracted thrice with CH_2Cl_2/water, and the CH_2Cl_2 phase was concentrated and precipitated thrice from cold diethyl ether. The obtained (PEO-Allyl-PEO)$_s$ was dried under vacuum at 45 °C for 24 h.

^{1}H NMR ($CDCl_3$) δ (ppm): 0.82 ppm (CH_3CH_2-), 1.22 ppm ($—OCH_2CH_2C—$), 1.37 ppm (CH_3CH_2-), 3.20–3.93 ppm ($—CH_2CH_2O—$), 4.72–4.74 ppm ($—OCH_2O—$), 5.07–5.27 ppm ($CH_2=CH—$), 5.79–5.91 ppm ($CH_2=CH—$). (See Figure S2 in Supporting Information) $M_{n,GPC} = 47{,}600$ g/mol, and PDI = 2.29.

Synthesis of Macroinitiator [PEO-(OH)$_2$-PEO]$_s$ by Thiol–Ene Addition Reaction (Scheme 2)

Using thiol–ene addition reaction, the allyl groups on (PEO-Allyl-PEO)$_s$ can be transformed into two hydroxyl groups. The (PEO-Allyl-PEO)$_s$ (7.00 g, 1.75 mmol), azobisisobutyronitrile (AIBN, 1.15 g, 7.00 mmol), and 1-thioglycerol (3.00 g, 27.70 mmol) were dissolved in 60 mL DMF in a 200 mL ampoule and degased by three freeze–thaw cycles at the temperature of liquid nitrogen. Then the system was charged with nitrogen and sealed, and the reaction was carried out at 60 °C for 48 h. After the solvent of DMF was eliminated under reduced pressure, the product was dissolved in distilled water and purified by ultrafiltration membrane separator to remove the small molecular residues. The final [PEO-(OH)$_2$-PEO]$_s$ product was obtained by direct evaporation of water and dried under vacuum at 45 °C for 24 h.

^{1}H NMR ($CDCl_3$) δ (ppm): 2.37–2.75 ppm ($—CH_2—S—CH_2—$) 3.20–3.93 ppm (m, $—CH_2CH_2O—$), 4.72–4.74 ppm ($—OCH_2O—$) (See Figure S3 in Supporting Information).

Synthesis of Graft Polymer PEO-*g*-PCL$_2$ by ROP Mechanism (Scheme 2)

The graft polymer PEO-*g*-PCL_2 was obtained by ROP of ε-CL monomers using [PEO-(OH)$_2$-PEO]$_s$ as macroinitiator. The [PEO-(OH)$_2$-PEO]$_s$ (1.00 g, 0.021 mmol) dried by azeotropic distillation with toluene, freshly distilled ε-CL (0.94 mL, 8.70 mmol), and $Sn(Oct)_2$ solution (0.17 mL, 0.21 mmol) was added into a 200-mL ampoule. After three freeze–thaw cycles at the temperature of liquid nitrogen, the system was charged with nitrogen and sealed, and the reaction was performed at 110 °C for 12 h. The final graft polymer PEO-*g*-PCL_2 was obtained by precipitation in petroleum ether and dried under vacuum at 45 °C for 24 h.

^{1}H NMR ($CDCl_3$) δ (ppm): 1.37 ppm ($—CH_2(CH_2)_2OC(=O)—$), 1.63 ppm ($—CH_2CH_2OC(=O)—$), 2.3 ppm ($—C(=O)CH_2—$), 3.20–3.93 ppm ($—CH_2CH_2O—$), 4.05 ppm ($—CH_2OC(=O)—$), 4.72–4.74 ppm ($—OCH_2O—$). (See Figure S4 in Supporting Information) $M_{n,GPC} = 131{,}000$ g/mol, and PDI = 1.92.

RESULTS AND DISCUSSION

Synthesis and Characterization of Macroinitiator [PEO-(OH)$_2$-PEO]$_s$

Using 3-[(allyloxy)methyl]-3-ethyl-1,5-pentanediol as initiator and DPMK as deprotonation agent, the precursor of PEO-Allyl-PEO with two active hydroxyl groups at chain end and one allyl group in middle position was synthesized by ROP mechanism. Figure 1(A) showed the GPC trace of PEO-Allyl-PEO ($M_{n,GPC} = 4800$ g/mol, PDI = 1.20), which showed a single peak with low PDI. From ^{1}H NMR spectrum of PEO-Allyl-PEO [Fig. 2(A)], the resonance signals at 3.25–3.83 ppm assigned to methylene protons ($—CH_2CH_2O—$) on EO units, and the characteristic signals at 5.06–5.26 and 5.79–5.91 ppm assigned to protons ($—CH_2=CH—$) and ($—CH_2=CH—$) on vinyl group were all well discriminated. The measurements of GPC and ^{1}H NMR clearly confirmed that the PEO-Allyl-PEO had been successfully synthesized. According to

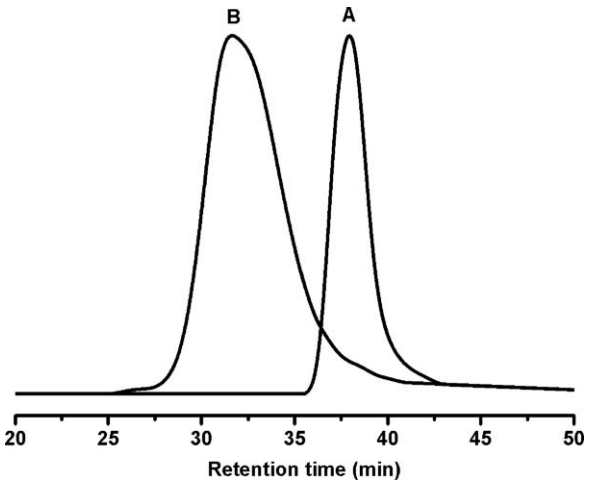

FIGURE 1 The GPC traces of (A) PEO-Allyl-PEO ($M_{n,GPC}$ = 4800 g/mol, PDI = 1.20) and (B) (PEO-Allyl-PEO)$_s$ ($M_{n,GPC}$ = 47,600 g/mol, PDI = 2.29).

^{1}H NMR spectrum [Fig. 2(A)], the accurate number average molecular weight of PEO-Allyl-PEO was also determined by Formula 1:

$$M_{n,NMR,PEO\text{-}Allyl\text{-}PEO} = \left(\frac{A_{d-h}/4}{A_a/3} \times 44\right) + 202. \quad (1)$$

Here, A_a represented the integral area of resonance signals for methyl protons (a) derived from initiator 3-[(allyloxy)-methyl]-3-ethyl-1,5-pentanediol, and A_{d-h} represented the sum of integral area of signals for methylene protons (d–h) derived from PEO chain.

Subsequently, the high-molecular-weight (PEO-Allyl-PEO)$_s$ was synthesized by Williamson reaction between active hydroxyl groups at the end of PEO-Allyl-PEO. Actually, the Williamson reaction was a rather efficient coupling reaction, which had been used as a cyclization method in our group[56] and literatures.[62–65] In this coupling reaction, CH_2Cl_2 was simultaneously used as coupling agent and solvent, and KOH was used as catalyst. To improve the basicity of reaction system and increase the molecular weight of (PEO-Allyl-PEO)$_s$, some NaH was also added. From the result of GPC for (PEO-Allyl-PEO)$_s$ ($M_{n,GPC}$ = 47,600 g/mol, PDI = 2.29) [Fig. 1(B)], the coupling extent can be evaluated about 10. From ^{1}H NMR spectrum for (PEO-Allyl-PEO)$_s$ shown in Figure 2(B), except for the characteristic resonance signals for methylene protons (—C***H***$_2$C***H***$_2$O—) on EO units, the signals of new formed acetal protons (—OC***H***$_2$O—) after coupling were also discriminated at 4.65–4.80 ppm.

To obtain the macroinitiator [PEO-(OH)$_2$-PEO]$_s$, the allyl groups on (PEO-Allyl-PEO)$_s$ were further transformed into hydroxyl groups by efficient thiol–ene addition reaction. During the modification procedure, DMF was used as solvent and AIBN was used as catalyst, and excess 1-thioglycerol was added to ensure that all the allyl groups were modified. After small molecular residues were removed by an ultrafiltration membrane using water as solvent, the pure [PEO-(OH)$_2$-PEO]$_s$ was obtained. As shown in Figure 2(C), the characteristic resonance signals at 5.07–5.27 and 5.79–5.91 ppm assigned to protons (C***H***$_2$═CH—) and (CH$_2$═C***H***—) on vinyl group were all disappeared, which confirmed that double bonds hanged on PEO main chain were all completely transformed into hydroxyl groups.

Thus, by the combination of ROP mechanism, efficient Williamson reaction, and thiol–ene addition reaction, we have successfully synthesized the macroinitiator [PEO-(OH)$_2$-PEO]$_s$ with modulated grafting sites.

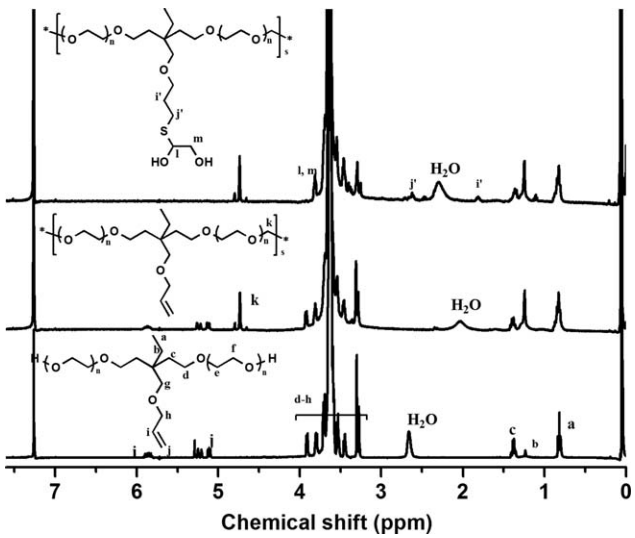

FIGURE 2 ^{1}H NMR spectra of (A) PEO-Allyl-PEO (in $CDCl_3$), (B) (PEO-Allyl-PEO)$_s$ (in $CDCl_3$), and (C) [PEO-(OH)$_2$-PEO]$_s$ (in $CDCl_3$).

Synthesis and Characterization of Graft Polymer PEO-*g*-PCL$_2$

By "grafting from" strategy, the target graft polymer PEO-*g*-PCL$_2$ with PEO as main chain and PCL as side chains was obtained by ROP of ε-CL monomers using [PEO-(OH)$_2$-PEO]$_s$ as macroinitiator and Sn(Oct)$_2$ as catalyst. Owing to the fast and reversibly transfer between hydroxyl groups and tin(II) alkoxide initiating species, the ROP was proceeded in a controlled style. By modulating the feed molar ratio of macroinitiator [PEO-(OH)$_2$-PEO]$_s$ to ε-CL monomers, a series of graft polymers PEO-*g*-PCL$_2$ with different lengths of PCL were obtained. In a typical ^{1}H NMR spectrum for PEO-*g*-PCL$_2$ (Fig. 3), except for the characteristic resonance signals for methylene protons (—C***H***$_2$C***H***$_2$O—) on EO units, the signals at 4.04, 2.30, 1.63, and 1.37 ppm attributed to the characteristic resonance signals on PCL side chains were all clearly discriminated. The GPC trace with a single peak also confirmed the successful synthesis of graft polymers (Fig. 4). The weight percentages of PCL on graft polymer were derived according to ^{1}H NMR spectra by Formula 2:

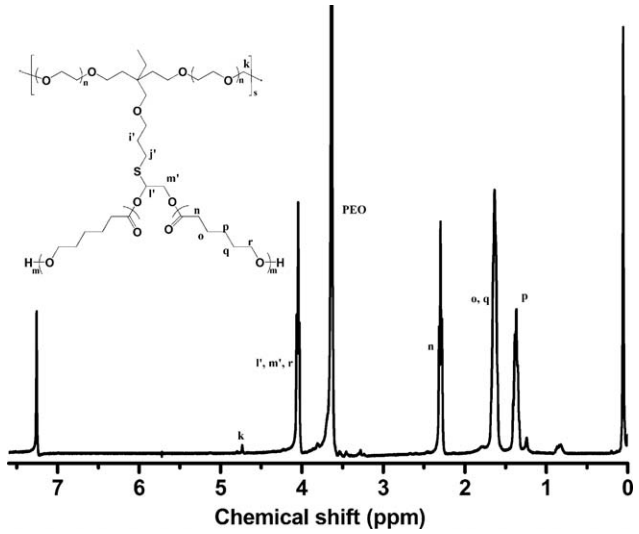

FIGURE 3 ^{1}H NMR spectrum of graft polymer PEO-*g*-PCL_2 (in $CDCl_3$).

$$W_{NMR,PCL}\% = \frac{(A_n/2)\times 114}{[(A_{d-h}/4)44]+[(A_n/2)114]}\times 100\%. \quad (2)$$

Here, A_n represented the integral area of signals for methylene protons (n) derived from PCL segments, and A_{d-h} represented the sum of integral area of signals for methylene protons (d–h) derived from PEO segments. The values of 114 and 44 were the molecular weight of ε-CL and EO monomer units, respectively.

Using the measurement of TGA, the compositions of graft polymers were also determined. As shown in Figure 5, the decomposition temperatures of the PEO and PCL segments could be discriminated clearly at 320 °C and 400 °C, respectively. According to the weight loss curves, we could calculate the weight percentages of PCL segments in graft polymers PEO-*g*-PCL_2, which were 9.90%, 40.1%, 55.0%, and 59.2%, respectively. These values ($W_{TGA,PCL}$) were rather consistent with those calculated from ^{1}H NMR spectra ($W_{NMR,PCL}$) (Table 1).

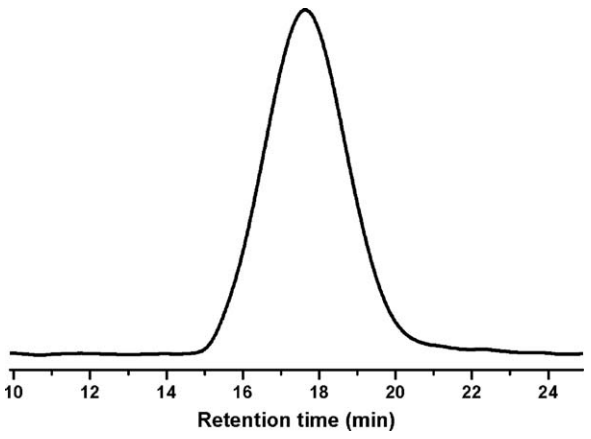

FIGURE 4 The GPC trace of graft polymer PEO-*g*-PCL_2 (a) ($M_{n,GPC}$ = 131,000 g/mol, PDI = 1.92).

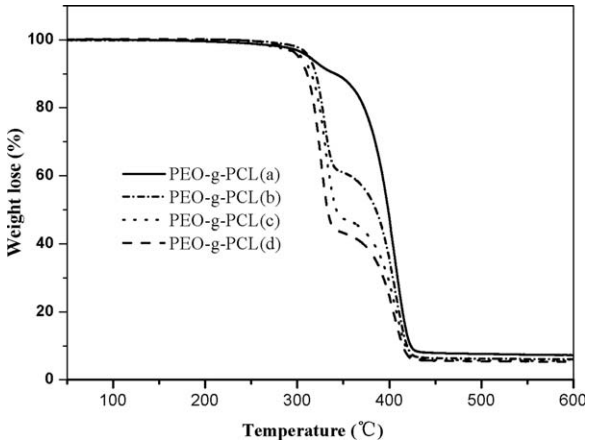

FIGURE 5 The TGA curves (10 °C/min) of PEO-*g*-PCL_2 under N_2 atmosphere.

Crystallization Behavior of Graft Polymer PEO-*g*-PCL_2

As both PEO backbone and PCL side chains are typical crystalline polymers, the theory of crystallization had been well investigated using PCL or PEO as separated objects.[66] Importantly, the polymers contained both PCL and PEO segments are especially worth to be investigated. Herein, the crystallization behavior of graft polymer PEO-*g*-PCL_2 with different PCL side chains was comprehensively studied by the measurements of DSC, XRD, and POM.

By the measurement of DSC (Fig. 6, Table 2), the crystallization temperature (T_c) was obtained from the cooling run, and the melting temperature (T_m) was obtained from the second heating run. For main chain [PEO-$(OH)_2$-PEO]$_s$, the T_c (33.64 °C) and T_m (47.08 °C) could be clearly discriminated. When PCL segments were grafted onto PEO main chain, for sample PEO-*g*-PCL_2 (a), because of the low PCL content (9.10%), only a T_c (28.24 °C) and a T_m (41.27 °C) assigned to PEO segments were observed, which were all slightly lower than that of main chain [PEO-$(OH)_2$-PEO]$_s$. When PCL content reached 40.1% [PEO-*g*-PCL_2 (b)], the T_c and T_m of PEO segment appeared at 25.82° and 42.69 °C, respectively. Simultaneously, a smaller peak assigned to the T_c of PCL segment could be observed at 7.50 °C. Continuously, when PCL content was increased to 54.5% [PEO-*g*-PCL_2 (c)], the T_cs of

TABLE 1 The Data for Graft Polymer PEO-*g*-PCL_2

Samples	$M_{n,GPC}$[a] (g/mol)	PDI[a]	$W_{TGA,PCL}$[b] (%)	$W_{NMR,PCL}$[c] (%)
PEO-*g*-PCL_2 (a)	131,000	1.92	9.90	9.10
PEO-*g*-PCL_2 (b)	167,000	1.96	40.1	40.1
PEO-*g*-PCL_2 (c)	186,000	2.3	55.0	54.5
PEO-*g*-PCL_2 (d)	304,000	2.41	59.2	59.2

[a] Determined by GPC using PMMA as standard and DMF as eluent.
[b] Calculated from TGA curves according to the respective weight loss of PCL and PEO segment.
[c] Calculated from ^{1}H NMR spectra according to Formula 2.

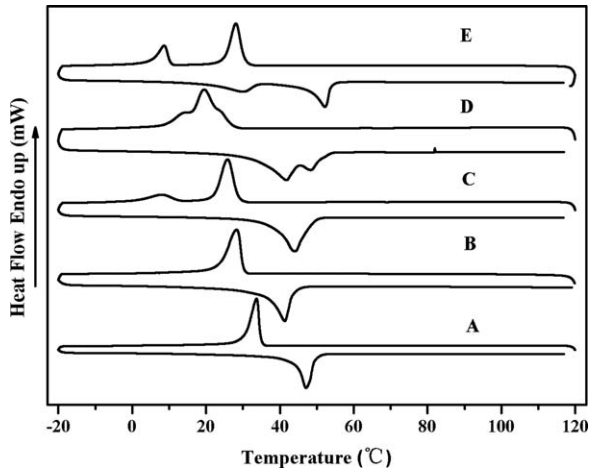

FIGURE 6 The DSC curves (10 °C/min) of (A) [PEO-$(OH)_2$-PEO]$_s$, (B) PEO-*g*-PCL_2 (a), (C) PEO-*g*-PCL_2 (b), (D) PEO-*g*-PCL_2 (c), and (E) PEO-*g*-PCL_2 (d) in the cooling run and the second heating run.

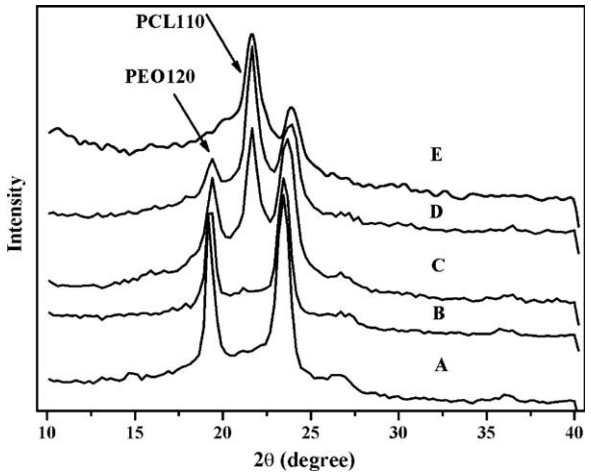

FIGURE 7 The XRD patterns of (A) [PEO-$(OH)_2$-PEO]$_s$, (B) PEO-*g*-PCL_2 (a), (C) PEO-*g*-PCL_2 (b), (D) PEO-*g*-PCL_2 (c), and (E) PEO-*g*-PCL_2 (d).

PCL and PEO, T_ms of PCL and PEO became approaching and almost mixed together, which were even difficult to be distinguished from each other. However, when PCL content reached 59.2% [PEO-*g*-PCL_2 (d)], the T_cs of PCL and PEO, T_ms of PCL and PEO were again separated. Especially, the T_c and T_m of PEO segments were lowered to 8.59° and 29.83 °C, whereas the T_c and T_m of PCL segments increased to 30.16° and 52.14 °C, respectively. Thus, the results of DSC confirmed that with the increase of PCL content, the dominant crystalline structure was changed from PEO part to PCL part. Furthermore, because of the surrounding of outer PCL segments to the inner PEO segments in graft polymers, when PCL content reached 59.2%, the crystalline of PEO segments had been largely suppressed. These results were obviously different from that of the literature.[66]

By the measurement of XRD, the crystallization behavior of PEO-*g*-PCL_2 was also studied, and all the samples were measured at room temperature without annealing. Typically, the linear PCL showed two intensive diffraction peaks at 21.6° and 23.9°,[67,68] and the linear PEO showed two intensive diffraction peaks at 19.1° and 23.3°, respectively.[69] As shown in Figure 7, the graft polymers PEO-*g*-PCL_2 also have the same diffraction peaks as that of PEO and PCL homopolymers. With the increase of PCL content in graft polymers, the diffraction peak at 19.1° corresponding to the (120) plane of the PEO crystallite became weaker. Simultaneously, the diffraction peak at 21.6° corresponding to the (110) plane of the PCL crystallite became stronger. When PCL content reached 59.2%, the crystalline structure of PEO part even could be neglected. Again, those results also showed that the crystalline structure was changed from PEO part to PCL part with the increase of PCL content, which were rather coincided with those of the results of DSC.

Furthermore, the crystallization behavior was also investigated by the measurement of POM (Fig. 8). From the POM micrograph of [PEO-$(OH)_2$-PEO]$_s$, we can observe the big spherulites of PEO segments clearly. When PCL segments were introduced, the crystallization behavior of graft polymer PEO-*g*-PCL_2 was significantly affected and modulated. From sample PEO-*g*-PCL_2 (a) to PEO-*g*-PCL_2 (d), the spherulites became smaller, which gradually tend to performance

TABLE 2 The DSC Data for [PEO-$(OH)_2$-PEO]$_s$ and Graft Polymer PEO-*g*-PCL_2

	T_c (°C)[a]		ΔH_c (J/g)[a]		T_m (°C)[b]		ΔH_m (J/g)[c]	
Samples	PEO	PCL	PEO	PCL	PEO	PCL	PEO	PCL
[PEO-$(OH)_2$-PEO]$_s$	33.64		87.39		47.08		92.03	
PEO-*g*-PCL_2 (a)	28.24		69.49		41.27		69.30	
PEO-*g*-PCL_2 (b)	25.82	7.50	50.31	13.60	42.76		60.98	
PEO-*g*-PCL_2 (c)	19.60		65.53		41.38	48.75	26.05	6.245
PEO-*g*-PCL_2 (d)	8.59	28.05	18.11	38.53	30.16	52.14	12.96	28.81

[a] T_c denotes the crystallization temperature of PEO or PCL segments in the cooling run.
[b] T_m denotes the melting point of PEO or PCL segments in the second heating run.
[c] ΔH_m denotes the fusion enthalpy of PEO or PCL segments in the second heating run.

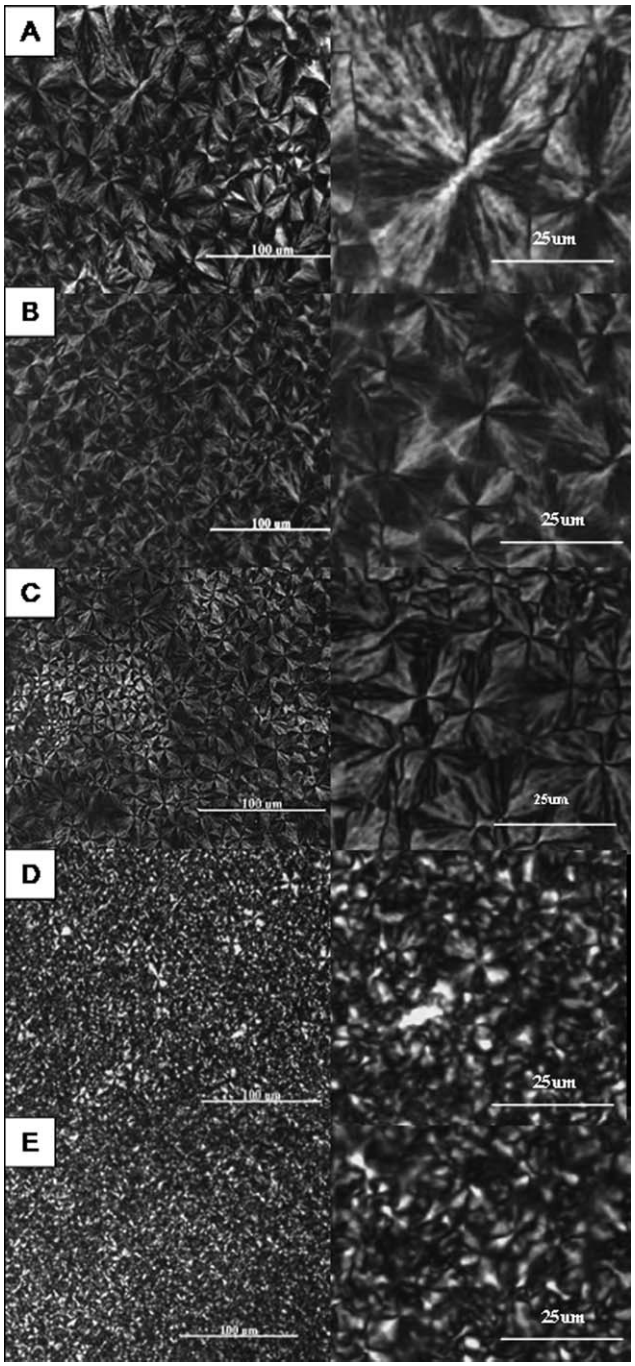

FIGURE 8 The POM micrographs for (A) $[PEO\text{-}(OH)_2\text{-}PEO]_s$, (B) PEO-*g*-$PCL_2$ (a), (C) PEO-*g*-PCL_2 (b), (D) PEO-*g*-PCL_2 (c), and (E) PEO-*g*-PCL_2 (d). The samples were prepared from 5% of chloroform solvent after 24 h of crystallization at room temperature.

and the characteristic crystallization behavior of PCL segments with the increase of PCL content.[66,70,71]

CONCLUSIONS

In this contribution, by the combination of ROP mechanism, Williamson reaction, with thiol–ene addition reaction, a series of graft polymers PEO-*g*-PCL_2 with modulated grafting sites were successfully synthesized. The target graft polymer and the intermediates were well characterized by the measurements of GPC, ^1H NMR, and TGA. By means of DSC, XRD, and POM, the crystallization behavior of the PEO-*g*-PCL_2 was also studied. Because of the grafted structure, when PCL content of side chains reached 59.2%, the crystalline structure had been dominated by PCL part and that of PEO part can almost be neglected. By the combination of the biodegradability with biocompatibility of both PEO and PCL segments, as well as the amphiphilicity, such graft polymers might be found some interesting applications in biomedical science, which are undergoing and will be presented in the future.

REFERENCES AND NOTES

1 V. S. Trubetskoy, *Adv. Drug Deliv. Rev.* **1999**, *37*, 81–88.

2 S. E. Stiriba, H. Kautz, H. Frey, *J. Am. Chem. Soc.* **2002**, *124*, 9698–9699.

3 R. Djalali, S. Y. Li, M. Schmidt, *Macromolecules* **2002**, *35*, 4282–4288.

4 M. Zhang, M. Drechsler, A. H. E. Muller, *Chem. Mater.* **2004**, *16*, 537–543.

5 L. H. He, J. Huang, Y. M. Chen, X. J. Xu, L. P. Liu, *Macromolecules* **2005**, *38*, 3845–3851.

6 Y. Q. Zhang, Z. Shen, D. Yang, C. Feng, J. H. Hu, G. L. Lin, X. Y. Huang, *Macromolecules* **2010**, *43*, 117–125.

7 N. Hadjichristidis, M. Pitsikalis, S. Pispas, H. Latrou, *Chem. Rev.* **2001**, *101*, 3747–3792.

8 S. J. Teertstra, M. Gauthier, *Prog. Polym. Sci.* **2004**, *29*, 277–327.

9 F. P. Yu, J. P. He, X. J. Wang, G. Z. Gao, Y. L. Yang, *J. Polym. Sci. Part A: Polym. Chem.* **2007**, *45*, 4013–4025.

10 A. X. Li, Z. J. Lu, Q. F. Zhou, F. Qiu, Y. L. Yang, *J. Polym. Sci. Part A: Polym. Chem.* **2006**, *44*, 3942–3946.

11 D. Uhrig, J. W. Mays, *Macromolecules* **2002**, *35*, 7182–7190.

12 X. Xiao, Y. G. Wu, M. H. Sun, J. J. Zhou, Z. S. Li, L. Bo, C. M. Chan, *J. Polym. Sci. Part A: Polym. Chem.* **2008**, *46*, 574–584.

13 P. Driva, D. J. Lohse, N. Hadjichristidis, *J. Polym. Sci. Part A: Polym. Chem.* **2008**, *46*, 1826–1842.

14 B. Helms, J. L. Mynar, C. J. Hawker, J. M. J. Frechet, *J. Am. Chem. Soc.* **2004**, *126*, 15020–15021.

15 Z. S. Bo, A. D. Schluter. *Chem. Eur. J.* **2000**, *6*, 3235–3241.

16 T. T. Tang, J. Huang, B. Huang, G. W. Wang, J. L. Huang, *J. Polym. Sci. Part A: Polym. Chem.* **2012**, *50*, 5144–5150.

17 G. W. Wang, X. S Fan, J. L. Huang, *J. Polym. Sci. Part A: Polym. Chem.* **2010**, *48*, 3797–3806.

18 Z. Y. Li, P. P. Li, J. L. Huang, *J. Polym. Sci. Part A: Polym. Chem.* **2006**, *44*, 4361–4371.

19 S. J. Teertstra, M. Gauthier, *Macromolecules* **2007**, *40*, 1657–1666.

20 G. Koutalas, D. J. Lohse, N. Hadjichristidis, *J. Polym. Sci. Part A: Polym. Chem.* **2005**, *43*, 4040–4049.

21 A. Hirao, H. Kawano, S. W. Ryu, *Polym. Adv. Technol.* **2002**, *13*, 275–284.

22 Y. G. Li, Y. Q. Zhang, D. Yang, Y. J. Li, J. H. Hu, C. Feng, S. J. Zhai, G. L. Lu, X. Y. Huang, *Macromolecules* **2010**, *43*, 262–270.

23 X. W. Xu, J. L. Huang, *J. Polym. Sci. Part A: Polym. Chem.* **2006**, *44*, 467–476.

24 H. Q. Xie, D. Xie, *Prog. Polym. Sci.* **1999**, *24*, 275–313.

25 R. Riva, S. Schmeits, C. Jerome, R. Jerome, P. Lecomte, *Macromolecules* **2007**, *40*, 796–803.

26 M. Schappacher, A. Deffieux, J. L. Putaux, P. Viville, R. Lazzaroni, *Macromolecules* **2003**, *36*, 5776–5783.

27 D. Neugebauer, Y. Zhang, T. Pakula, S. S. Sheiko, K. Matyjaszewski, *Macromolecules* **2003**, *36*, 6746–6755.

28 W. Z. Yuan, J. Y. Yuan, M. Zhou, X. F. Sui, *J. Polym. Sci. Part A: Polym. Chem.* **2006**, *44*, 6575–6586.

29 Q. Fu, W. C. Lin, J. L. Huang, *Macromolecules* **2008**, *41*, 2381–2387.

30 R. M. Sun, G. W. Wang, C. Liu, J. L. Huang, *J. Polym. Sci. Part A: Polym. Chem.* **2009**, *47*, 1930–1938.

31 W. C. Lin, Q. Fu, Y. Zhang, J. L. Huang, *Macromolecules*, **2008**, *41*, 4127–4135.

32 R. Djalali, N. Hugenberg, K. Fischer, M. Schmidt, *Macromol. Rapid Commun.* **1999**, *20*, 444–449.

33 V. Heroguez, Y. Gnanou, M. Fontanille, *Macromolecules* **1997**, *30*, 4791–4798.

34 L. N. Gu, Z. Shen, G. L. Lu, X. H. Zhang, X. Y. Huang, *Macromolecules* **2007**, *40*, 4486–4493.

35 U. Tunca, *Macromol. Rapid Commun.* **2013**, *34*, 38–46.

36 U. S. Gunay, B. Ozsoy, H. Durmaz, G. Hizal, U. Tunca, *J. Polym. Sci. Part A: Polym. Chem.* **2013**, *51*, 4667–4674.

37 H. Durmaz, A. Sanyal, G. Hizal, U. Tunca, *Polym. Chem.* **2012**, *3*, 825–835.

38 D. A. Herold, K. Keil, D. E. Bruns, *Biochem. Pharmacol.* **1989**, *38*, 73–76.

39 S. Jain, F. S. Bates, *Macromolecules* **2004**, *37*, 1511–1523.

40 C. X. Cheng, Y. Huang, R. P. Tang, E. Q. Chen, F. Xi, *Macromolecules* **2005**, *38*, 3044–3047.

41 P. Jannasch, *Macromolecules* **2000**, *33*, 8604–8610.

42 K. E. Uhrich, S. M. Cannizzaro, R. S. Langer, K. M. Shakesheff, *Chem. Rev.* **1999**, *99*, 3181–3198.

43 W. Chen, Y. Zou, J. N. Jia, F. H. Meng, R. Cheng, C. Deng, F. J. Jan, Z. Y. Zhong, *Macromolecules* **2013**, *46*, 699–707.

44 H. Freichels, V. Pourcelle, R. Auzely-Velty, J. Marchand-Brynaert, C. Jerome, *Biomacromolecules* **2013**, *13*, 760–768.

45 H. Y. Li, R. Riva, R. Jerome, P. Lecomte, *Macromolecules* **2007**, *40*, 824–831.

46 R. K. Jing, G. W. Wang, J. L. Huang, *J. Polym. Sci. Part A: Polym. Chem.* **2010**, *48*, 5430–5438.

47 Q. Fu, C. Liu, W. C. Lin, J. L. Huang, *J. Polym. Sci. Part A: Polym. Chem.* **2008**, *46*, 6770–6779.

48 G. W. Wang, Y. N. Zhang, J. L. Huang, *J. Polym. Sci. Part A: Polym. Chem.* **2010**, *48*, 1633–1640.

49 P. P. Li, Z. Y. Li, J. L. Huang, *Macromolecules* **2007**, *40*, 491–498.

50 P. P. Li, Z. Y. Li, J. L. Huang, *Polymer* **2007**, *48*, 1557–1566.

51 Z. Y. Li, P. P. Li, J. L. Huang, *Polymer* **2006**, *47*, 5791–5798.

52 J. Huang, Z. Y. Li, X. W. Xu, Y. Ren, J. L. Huang, *J. Polym. Sci. Part A: Polym. Chem.* **2006**, *44*, 3684–3691.

53 X. L. Luo, G. W. Wang, X. C. Pang, J. L. Huang, *Macromolecules* **2008**, *41*, 2315–2317.

54 G. W. Wang, X. L. Luo, Y. N. Zhang, J. L. Huang, *J. Polym. Sci. Part A: Polym. Chem.* **2009**, *47*, 4800–4810.

55 X. C. Pang, G. W. Wang, X. F. Jia, C. Liu, J. L. Huang, *J. Polym. Sci. Part A: Polym. Chem.* **2007**, *45*, 5824–5837.

56 X. C. Pang, R. K. Jing, J. L. Huang, *Polymer* **2008**, *49*, 893–900.

57 Z. F. Jia, Q. Fu, J. L. Huang, *Macromolecules* **2006**, *39*, 5190–5193.

58 J. W. Mays, D. Uhrig, S. Gido, Y. Q. Zhu, R. Weidisch, H. Iatrou, N. Hadjichristidis, K. Hong, F. Beyer, R. Lach, M. Buschnakowski, *Macromol. Symp.* **2004**, *215*, 111–126.

59 H. Iatrou, J. W. Mays, N. Hadjichristidis, *Macromolecules* **1998**, *31*, 6697–6701.

60 M. Vert, S. M. Li, G. Splenehauer, P. Guerin, *J. Mater. Sci.: Mater. Med.* **1992**, *3*, 432–446.

61 R. Francis, D. Taton, J. L. Logan, P. Masse, Y. Gnanou, R. S. Duran, *Macromolecules* **2003**, *36*, 8253–8259.

62 J. Cooke, K. Viras, G. E. Yu, T. Sun, T. Yonemitsu, A. J. Ryan, C. Price, C. Booth, *Macromolecules* **1998**, *31*, 3030–3039.

63 T. Sun, G. E. Yu, C. Price, C. Booth, J. Cooke, A. J. Ryan, *Polymer* **1995**, *36*, 3775–3778.

64 Z. G. Yan, Z. Yang, C. Price, C. Booth, *Makromol. Chem. Rapid Commun.* **1993**, *14*, 725–732.

65 G. Yu, P. Sinnathamby, C. Price, C. Booth, *Chem. Commun.* **1996**, *1*, 31–32.

66 C. L. He, J. R. Sun, J. Ma, X. S. Chen, X. B. Jing, *Biomacromolecules* **2006**, *7*, 3482–3489.

67 L. Wang, J. L. Wang, C. M. Dong, *J. Polym. Sci. Part A: Polym. Chem.* **2005**, *43*, 4721–4730.

68 L. Chen, Y. S. Ni, X. C. Bian, X. Y. Qiu, X. L. Zhuang, X. S. Chen, X. B. Jiang, *Carbohydr. Polym.* **2005**, *60*, 103–109.

69 G. Maglio, G. Nese, M. Nuzzo, R. Palumbo, *Macromol. Rapid Commun.* **2004**, *25*, 1139–1144.

70 C. L. He, J. R. Sun, T. Zhao, Zh. K. Hong, X. L. Zhuang, X. S. Chen, X. B. Jing, *Biomacromolecules* **2006**, *7*, 252–258.

71 C. L. He, J. R. Sun, C. Deng, T. Zhao, M. X. Deng, X. S. Chen, X. B. Jing, *Biomacromolecules* **2004**, *5*, 2042–2047.